

20. The presence of boulders with a span of exposure ages (~34 to 22 ky B.P.) on the LLGM moraines may mean that glacier termini remained close to their maxima for up to ~12,000 years or fluctuated, building composite moraines. It is also possible that younger ages represent the effects of boulder exhumation, movement, or differential boulder erosion.
21. R. Müller, thesis, University of Zürich (1985).
22. M. Stute *et al.*, *Science* **269**, 379 (1995).
23. D. W. Lea, D. K. Pak, H. J. Spero, *Science* **289**, 1719 (2000).
24. J. Oerlemans, in *Glacier Fluctuations and Climatic Change*, J. Oerlemans, Ed. (Kluwer Academic, Dordrecht, Netherlands, 1989), pp. 353–371.
25. D. H. Clark, M. M. Clark, A. R. Gillespie, *Quat. Res.* **41**, 139 (1994).
26. A. M. Johnson, in *World Survey of Climatology*, Vol. 12, W. Schwerdtfeger, Ed. (Elsevier, New York, 1976), pp. 147–218.
27. S. C. Fritz *et al.*, *Quat. Res.* **61**, 95 (2004).
28. P. A. Baker *et al.*, *Nature* **409**, 698 (2001).
29. J. Imbrie *et al.*, in *Milankovitch and Climate, Part 1*, A. L. Berger, J. Imbrie, J. Hays, G. Kukla, B. Saltzman, Eds. (Reidel, Dordrecht, Netherlands, 1984), pp. 269–305.
30. L. A. Owen *et al.*, *Quat. Sci. Rev.*, in press.
31. G. D. Thackray, *Quat. Res.* **55**, 257 (2001).
32. T. V. Lowell, *Quat. Sci. Rev.* **14**, 85 (1995).
33. We acknowledge financial and/or material support from the National Geographic Society (grant 7188-02), Lawrence Livermore National Laboratory, the Geological Society of America, Union College, Syracuse University, and NSF (grant ATM-0081517). We are grateful to two

anonymous reviewers whose comments and suggestions substantially improved the manuscript. We dedicate this report to the memory of our coauthor, colleague, and friend, Geoff Seltzer, who was an integral part of the project from beginning to end.

#### Supporting Online Material

www.sciencemag.org/cgi/content/full/308/5722/678/DC1

Materials and Methods

SOM Text

Figs. S1 and S2

Table S1

References

3 November 2004; accepted 25 February 2005

10.1126/science.1107075

# Laboratory Earthquakes Along Inhomogeneous Faults: Directionality and Supershear

Kaiwen Xia,<sup>1,2\*</sup> Ares J. Rosakis,<sup>1†</sup> Hiroo Kanamori,<sup>2</sup> James R. Rice<sup>3</sup>

We report on the experimental observation of spontaneously nucleated ruptures occurring on frictionally held bimaterial interfaces with small amounts of wave speed mismatch. Rupture is always found to be asymmetric bilateral. In one direction, rupture always propagates at the generalized Rayleigh wave speed, whereas in the opposite direction it is subshear or it transitions to supershear. The lack of a preferred rupture direction and the conditions leading to supershear are discussed in relation to existing theory and to the earthquake sequence in Parkfield, California, and in North Anatolia.

There is evidence for supershear rupture propagation during earthquakes (1–6), and the link between large earthquakes and the conditions leading to supershear has been established experimentally (7).

Although many of the physical aspects of dynamic rupture (including supershear) are recently becoming clearer in relation to homogeneous faults (i.e., faults separating the same material) (7–13), the behavior of spontaneously nucleated ruptures in inhomogeneous faults (i.e., separating materials with different wave speeds) is still experimentally unexplored except in (14). Because many large earthquakes rupture on faults separating rock masses with different wave speeds, the mechanics of sliding in bimaterial systems is relevant to seismology. Specifically, the questions of whether a preferred rupture direction exists (11), whether a unilateral or bilateral faulting dominates (15), and what the condition is for supershear rupture propagation are particularly relevant to fault dynamics. These questions are

also relevant to hazard potentials of large earthquakes, because directionality and rupture speed control near-field ground motions.

According to analysis and numerics, there are two types of such steady, self-sustained pulses (16, 17). One type corresponds to rupture growth in the direction of slip in the lower wave speed material of the system, and this direction is referred to as the positive direction (10, 11). The rupture pulses belonging to this type are subshear and always propagate with a steady velocity  $V = +C_{GR}$ , the generalized Rayleigh (GR) wave speed of the system. In this work, we refer to such ruptures as positive GR ruptures and abbreviate them as +GR ruptures. The second type of self-sustained ruptures corresponds to propagation in the negative direction opposite to +GR ruptures (17, 18). Such pulses are supershear and always propagate with a steady velocity that is slightly lower than the  $P$ -wave speed of the material with the lower wave speed ( $V = -C_p^2$ ). In the present paper, we will abbreviate such ruptures as  $-P_{SLOW}$  ruptures.

Our experiments examined the effect of material contrast on the rupture growth of spontaneously nucleated dynamic ruptures hosted by inhomogeneous, frictional interfaces. These interfaces are held together by static, far-field pressure-shear simulating natural tectonic loads. The experiments mimic natural earthquakes where bimaterial contrast between intact rock masses seldom exceeds

30% in shear wave speeds (10). The experimental setup is similar to that used in our previous study of rupture in homogeneous interfaces (7). This configuration has proven effective in producing accurate, full-field, and real-time information of generic rupture characteristics that can ultimately be related to the rupture behavior of natural fault systems.

A Homalite-100 [Homalite (Division of BIG, Incorporated), Wilmington, DE] plate (material 1, top) and a polycarbonate plate (material 2, bottom) are held together by far-field load,  $P$  (Fig. 1). The ratio of shear wave speeds in the materials,  $C_S^1/C_S^2 = 1.25$ , is chosen to be at the high end of the naturally occurring bimaterial range so that the interfacial phenomena of interest are observable in the experiments. The shear wave speeds (Fig. 1) are directly measured for each material by following the shear wave fronts with the use of high-speed photography and photoelasticity. Photoelasticity, being sensitive to maximum shear stress fields, is perfectly suited for measuring shear wave speeds and for scrutinizing shear-dominated rupture processes in brittle, transparent, and birefringent solids (7). The  $P$ -wave speeds were calculated by using measured values of Poisson's ratios ( $\nu^1 = 0.35$ ,  $\nu^2 = 0.38$ ) and by using the directly measured shear wave speeds. Plain strain values were used, because we are interested in processes that take place at short wavelengths near the front of the rupture. An independent measurement of the longitudinal wave ( $P$  wave) speeds in the plates using ultrasonic transducers has confirmed these calculated values to within 5%. GR waves for this bimaterial pair exist, and their speed is calculated to be  $C_{GR} = 959$  m/s, a value which is close to the shear wave speed of polycarbonate.

The dynamic rupture is triggered by means of an exploding wire mechanism, which simulates a localized pressure release at the desired location of the simulated hypocenter (7). About 32 experiments featuring different angles,  $\alpha$  ( $20^\circ$ ,  $22.5^\circ$ , and  $25^\circ$ ), and far-field loading  $P$  (10, 13, and 18 MPa) were performed, and the rupture events were repeatedly visualized in intervals of 3  $\mu$ s by a digital high-speed camera system used in conjunction with dynamic photoelasticity (7).

<sup>1</sup>Graduate Aeronautical Laboratories, California Institute of Technology (Caltech), Pasadena, CA 91125, USA. <sup>2</sup>Seismological Laboratory, Caltech, Pasadena, CA 91125, USA. <sup>3</sup>Division of Engineering and Applied Sciences and Department of Earth and Planetary Sciences, Harvard University, Cambridge, MA 02138, USA.

\*Present address: Division of Engineering, Brown University, Box D, Providence, RI 02912, USA.

†To whom correspondence should be addressed. E-mail: rosakis@aero.caltech.edu

The higher level of angles was limited by the static frictional characteristics of the interface. Depending on  $P$  and  $\alpha$ , three distinct and repeatable rupture behaviors were observed. In all cases, the two separate, semi-circular traces of the shear waves in the two materials were visible as discontinuities in the maximum shear stress field. The ruptures were always bilateral and became progressively asymmetric with time within the time window of all experiments.

Two distinct rupture tips, one propagating to the west and the other to the east with velocities  $V^E$  and  $V^W$ , respectively, were identified by a distinct concentration of fringe lines (Fig. 2). For this case (case 1), both tips propagated at subshear velocities,  $V^E < V^W < C_S^1 < C_S^2$ . Differentiation of the rupture length time histories, obtained from a series of high-speed images, allows for estimation of the rupture velocity histories. The rupture propagating to the west is in the direction of slip of the lower wave speed material (positive direction). Within experimental error, this rupture is found to propagate at a constant velocity close to  $C_{GR}$  ( $V^W = 950 \text{ m/s} \approx +C_{GR}$ ). The rupture propagating to the east (negative direction) grows at an almost constant subshear velocity  $V^E = -900 \text{ m/s}$ , which is slower than the Rayleigh wave speed,  $C_R^2$ , in the slower wave speed material. The observations were similar for smaller  $\alpha$  values and compressive  $P$  loads as well. In this case, the rupture speed to the east remained sub-Rayleigh ( $V^E < C_R^1 < C_R^2$ ). However, its velocity varied continuously across experiments with different load levels and angles. In particular, smaller  $\alpha$  and lower  $P$  resulted in  $V^E$  being lower fractions of  $C_R^2$ .

A distinct but equally repeatable rupture case (case 2) was observed for higher values of  $\alpha$  and  $P$ . These conditions correspond to higher values of driving stress or to conditions closer to incipient uniform sliding of the entire interface. A typical example corresponding to  $\alpha = 25^\circ$  and  $P = 18 \text{ MPa}$  (Fig. 3) shows that the rupture was bilateral with a westward tip trailing behind both shear wave traces. This tip propagated at a constant velocity  $V^W \approx +C_{GR}$ . This observation is identical to the situation described above in relation to lower values of  $\alpha$  and  $P$ . The eastward propagating tip, however, is different from the previously described case. This tip propagated with a velocity faster than both the shear wave speeds. Moreover, its structure (Fig. 3) is distinctly different from the structure of westward moving +GR type of rupture. As a conclusive proof of its supershear velocity, two distinct shear shock waves are clearly visible. The magnitude of the velocity of the eastward rupture  $|V^E|$  was  $1920 \text{ m/s}$ , which is  $\sim 12\%$  less than the longitudinal wave ( $P$  wave) speed,  $C_P^2$ , of the

lower wave speed material.  $|V^E|$  is also equal to  $1.6C_S^1$  or is slightly higher than  $\sqrt{2} C_S^2$ .

Both cases described above feature westward propagating ruptures that are of the +GR type. Irrespective of the values of  $\alpha$  and  $P$ , these ruptures have a constant speed  $V^W \approx +C_{GR}$  and they propagate in the positive direction. However, those two cases also feature eastward ruptures that are distinctly different in nature. For sufficiently low  $P$  and  $\alpha$ , the eastward ruptures, which propagate in the negative direction, are purely subshear within the time window of our experiments. For large enough  $P$  and  $\alpha$ , however, eastward ruptures propagate with a constant supershear velocity whose magnitude is slightly less than  $C_P^2$  and are thus of the  $-P_{SLOW}$  type. To visualize an intermediate situation and a controlled transition from one case to the other within the field of view, we reduced  $P$  to  $13 \text{ MPa}$  (Fig. 4, A and B). Indeed for this case (case 3), Fig. 4 shows a smooth transition from case 1 to case 2 within the same experiment. Although the westward rupture remains of the +GR type throughout the experiment, the eastward rupture jumps from a constant subshear velocity ( $-910 \text{ m/s}$ ) to a constant supershear velocity ( $-1920 \text{ m/s}$ ) and thus transitions to the  $-P_{SLOW}$  type. The rupture length-versus-time plot (Fig. 5) also shows the abrupt transition of the eastward rupture from a subshear velocity to a velocity whose magnitude is slightly less than  $C_P^2$ . This happens at a transition length,  $L$ , which is  $\sim 25 \text{ mm}$ .

The eastward transition behavior of case 3 (Figs. 4 and 5) is similar to the one we have discussed (7) in relation to homogeneous interfaces, whereas the transition length,  $L$ , is also a decreasing function of  $\alpha$  and  $P$ . The ruptures that propagate in the negative direction require a certain minimum rupture length before they become supershear. This observation suggests a link between supershear growth in the negative direction and large earthquakes. In contrast, no such transition was observed for +GR ruptures, irrespective of  $\alpha$ ,  $P$ , and rupture length.

Although it is difficult to determine whether the ruptures are pulse-like, crack-like, or a mixture of the two, the observations confirm the existence of two distinct self-sustained and constant speed rupture modes. These are similar to the ones that have been theoretically and numerically predicted (10, 11, 17, 19–21). In particular, a +GR type of rupture mode is always excited instantaneously in the positive direction. Furthermore, a  $-P_{SLOW}$  mode is observed as long as the rupture propagating in the negative direction is allowed to grow to sufficiently long distances from the hypocenter. The triggering of the  $-P_{SLOW}$  mode is always preceded by a purely subshear, crack-like rupture whose velocity depends on loading and geometry as well as on the bi-

material characteristics. Therefore, the existence of this preliminary and apparently transient stage is one of the main differences with early numerical and theoretical predictions (11, 16, 17, 19, 20, 22, 23).

Another difference from some of the numerical predictions (11, 17, 20, 21) is the consistent experimental observation of bilateral rupturing. In contrast to the experiments, the above numerical predictions only excite one or the other of the two self-sustained rupture modes (17), giving rise to purely unilateral rupture events. They also favor the triggering of the +GR mode in low wave speed mismatch bimaterial systems (11, 20). This kind of preference has led to the labeling of the positive direction as the preferred rupture direction (11). These numerical results are also consistent with the notion of rupture directionality (15), whereas our experiments are not. One exception to this rule is provid-

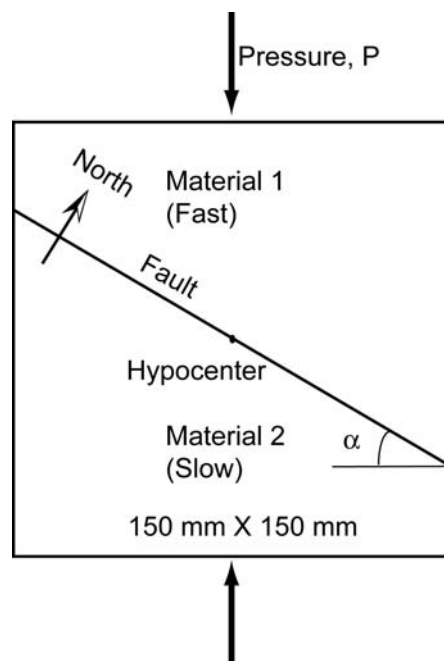


**Fig. 1.** Laboratory earthquake model composed of two photoelastic plates of the same geometry. The higher wave speed material at the top (Homalite-100) has a density  $\rho_1 = 1262 \text{ kg/m}^3$ , a shear wave speed  $C_S^1 = 1200 \text{ m/s}$ , and a longitudinal wave speed  $C_P^1 = 2,498 \text{ m/s}$ . The lower wave speed material at the bottom (polycarbonate) has a density  $\rho_2 = 1192 \text{ kg/m}^3$ , a shear wave speed  $C_S^2 = 960 \text{ m/s}$ , and a longitudinal wave speed  $C_P^2 = 2,182 \text{ m/s}$ . The fault is simulated by a frictionally held contact interface with an angle to the applied load, which is varied to mimic a wide range of tectonic load conditions. Spontaneous rupture is triggered at the hypocenter through an exploding wire mechanism. The static compressive load  $P$  is applied through a hydraulic press. By arbitrary convention, the fault strike runs in the east-west direction with the lower wave speed solid located on the south side. As viewed from the camera, a rupture will produce right lateral slip.

ed by the early numerical analysis by Harris and Day (24), which consistently reports asymmetric bilateral rupture growth in a variety of low speed contrasts in homogeneous fault systems. The results of Harris and Day are qualitatively similar to the experimental observations of cases 1 and 2. However, no transition is reported. To reconcile the observed differences between models and our experiments, we note that unstable slip rupture propagation has also been observed (7) on Homalite/Homalite and polycarbonate/polycarbonate interfaces. Such unstable rupture growth would be possible only if there was a reduction of friction with slip and/or slip rate, and hence such reduction must be a property of both materials when sliding against themselves. It is then plausible to assume that a similar reduction of friction occurs along the Homalite/polycarbonate interface. Hence, its rupture behavior should not be expected to fully correspond to the idealized models of a dissimilar material interface with constant coefficient of friction. Indeed the goal of some of the early theoretical and numerical studies (10, 11, 16, 17, 19, 20, 22, 23) was to investigate what kind of unstable slip would develop on a surface that, as judged from conventional friction notions, was superficially stable in the sense that its friction coefficient,  $f$ , did not decrease with slip and/or slip rate. For most brittle solids, however, ample evidence exists that  $f$  does decrease with increase of slip and/or slip rate. As a result, a proper model for natural faulting along a bimaterial interface should include both a weakening of  $f$  and the slip-normal stress coupling effects of the bimaterial situation. Indeed, such a weakening model

was included by Harris and Day (24). Given the above, it would be an invalid interpretation of the results of the earlier set of papers to conclude that the rupture (including preference for specific rupture mode) scenarios they predict constitute the full set of scenarios available to a real earthquake, of which  $f$  decreases with increasing slip and/or slip rate. The consistently bilateral nature of rupture predicted by Harris and Day (24) is perhaps an indication of the effect of including a slip weakening frictional law in their calculations.

Our experiments do not support a preference of rupture direction. Although they support the idea that frictional ruptures in the positive direction always propagate at a specific constant velocity ( $V = +C_{GR}$ ), they still allow for self-sustained intersonic ruptures eventually growing in the negative direction. This possibility becomes more likely if their transient, subshear, and precursory ruptures propagate over a long enough distance and are not arrested prior to transitioning to supershear. The requirement of a critical transition length in the negative direction thus provides a link between large earthquakes and the occurrence of self-sustained supershear rupture in the negative direction.

The 1999, M7.4, Izmit earthquake in Turkey is perhaps a good example for which both modes of self-sustained rupture may have been simultaneously present, as is the case in our experiments. The event was a right-lateral bilateral rupture on a straight segment of the North Anatolian fault. The westward propagating rupture had a speed close to the Rayleigh wave speed, whereas the eastward rupture had a supershear speed that was slightly above the  $\sqrt{2}$  times the shear wave

speed of crustal rock (3, 25). Because the geometry of our laboratory earthquake is similar to the Izmit event, direct comparison of the Izmit earthquake and the case described in Fig. 3 reveals similarities. In addition to the right lateral asymmetric bilateral rupture, case 2 featured a subshear westward rupture propagating at  $+C_{GR}$ . To the east, however, the laboratory rupture propagated at a velocity whose magnitude was slightly lower than  $C_{GR}^2$ , which also happens to be equal to  $1.6C_S^1$  for the particular bimaterial contrast of the experiments. Indeed, if one interprets the Izmit event as occurring in an inhomogeneous fault with the lower wave speed material being situated at the southern side of the fault, the field observations and the experimental measurements of both rupture directions and speeds are consistent. Moreover, when the bimaterial contrast is low enough, the differences between  $C_{GR}$  and the average of the two Rayleigh wave speeds,  $(C_R^1 + C_R^2)/2$ , as well as the difference between  $1.6C_S^1$  and  $\sqrt{2}(C_S^1 + C_S^2)/2$ , would be small enough not to be distinguished by the inversion process. In addition, viewing the fault as inhomogeneous can explain the choice of direction for the subshear and the supershear branches, respectively (26). The 1999 Düzce earthquake can also be interpreted along a similar line of argument as used for Izmit. The Düzce rupture featured right lateral slip, and it extended the Izmit rupture zone 40 km eastward through asymmetric bilateral slip (3). Modelling indicates subshear westward and supershear eastward rupture fronts. The direct comparison with case 2 (Fig. 3) thus provides an explanation for the rupture direction and velocity. This explana-

**Fig. 2. (Left)** Rupture case 1. The photoelastic patterns for an experiment with  $\alpha = 22.5^\circ$  and  $P = 18$  MPa. Both ruptures to the east and the west are subshear. **Fig. 3. (Right)** Rupture case 2. For  $\alpha = 25^\circ$  and  $P = 18$  MPa, the bilateral rupture features two distinct tips. The one propagating to the west (positive direction) has a velocity  $V^W \approx +C_{GR}$ , whereas the one propagating to the east (negative direction) is supershear ( $V^E$ ). (Upper insert) Two clear lines of discontinuity in the maximum shear contours of photoelasticity. Each of these lines

(shear shock waves) is located at two different angles,  $\beta_1 = 41^\circ$  and  $\beta_2 = 30^\circ$ , to the north and to the south of the fault, respectively. The two angles,  $\beta_n$ ,  $n = 1, 2$ , are related to the shear wave speeds  $C_S^n$  and to the rupture velocity  $V^E$ , by  $\beta_n = \sin^{-1}(V^E/C_S^n)$ . This relation

provides independent means of estimating  $V^E$  from each individual frame of the high speed camera record without reliance on the less accurate rupture length history. Both methods yield consistent values of  $V^E = -1920$  m/s.

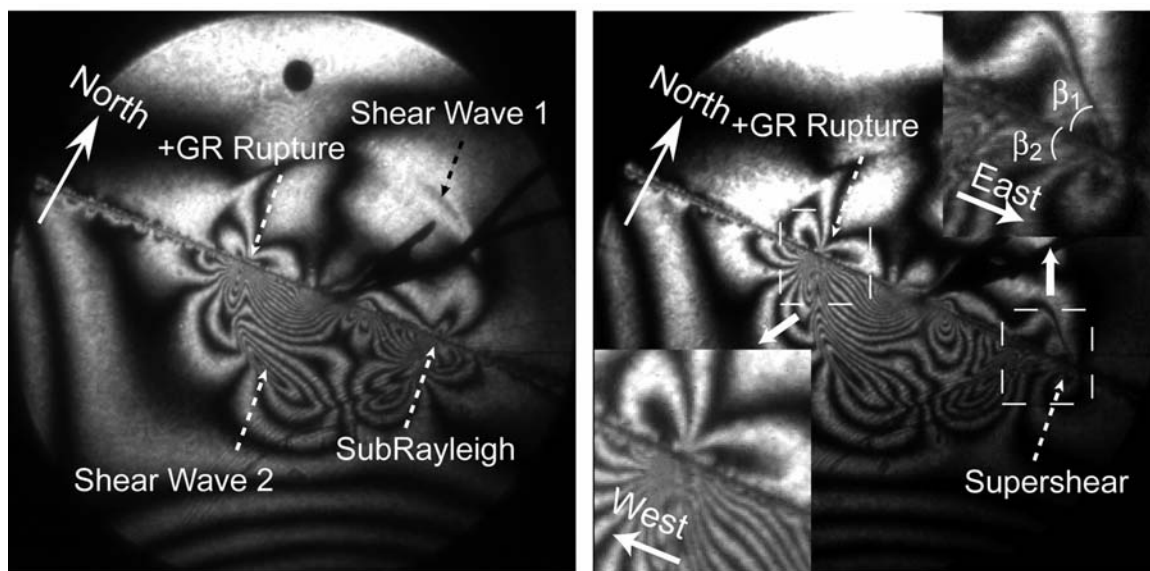


**Fig. 4.** Rupture case 3. Experimental results for  $\alpha = 25^\circ$  and  $P = 13$  MPa showing transition of the eastward-moving rupture to supershear. The westward rupture retains a constant velocity  $V^W \approx +C_{GR}$ . (A) Before transition to supershear. (B) After transition to supershear.

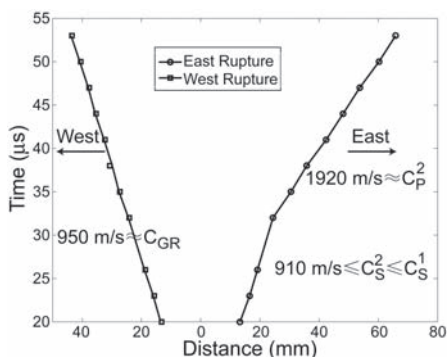
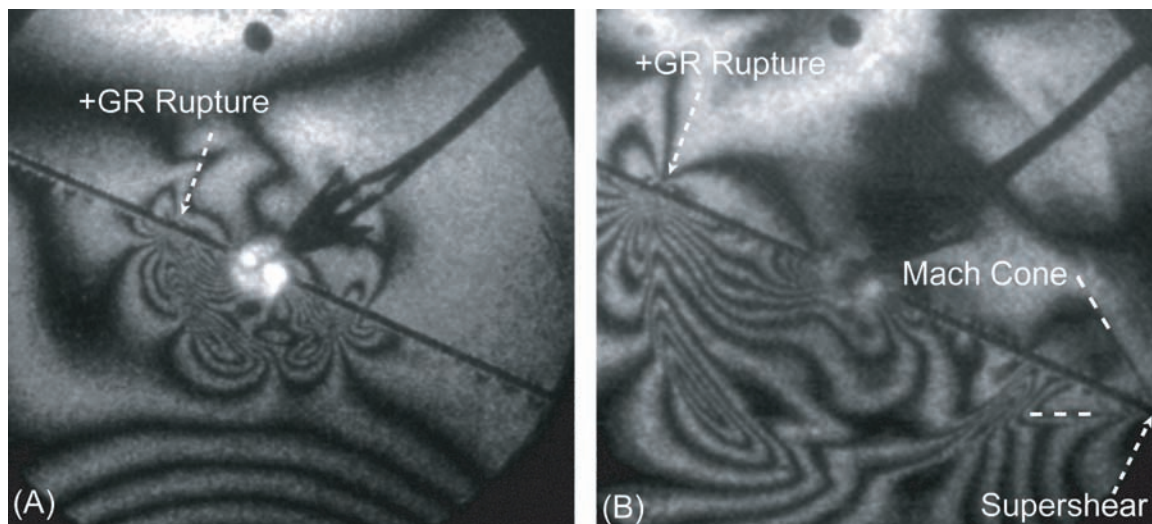


**Fig. 5.** Rupture time-distance plot for an experiment with  $\alpha = 25^\circ$  and  $P = 13$  MPa.

tion is plausible if one assumes that the material to the south of the North Anatolian fault, at its western end, is the lower wave speed solid.

By using similar arguments to the ones used for Izmit and Düzce, one can perhaps provide a unified rationalization of the seemingly random rupture directions and rupture velocities of the series of earthquakes that have occurred since 1939 along the North Anatolian fault and ended in 1999 with the Izmit and Düzce events. The following argument requires the assumption that, in average and along its entire length, the North Anatolian fault features the same type of bimaterial inhomogeneity as the one that has been summarized for Izmit and Düzce. Limited evidence supporting such an assumption is currently available (27). If this is true, in some average sense, one would expect that the slight majority (60%) of the large ( $M \geq 6.8$ ) earthquake events (i.e., 1939-M7.9, 1942-M6.9, 1944-M7.5, 1951-M6.8, 1957-M6.8, and 1967-M7.0), which featured westward propagating ruptures, were probably of the +GR type. In other words, that implies that they were classical subshear ruptures that

propagated at  $+C_{GR}$  in the positive direction. The remaining four ruptures (i.e., 1943-M7.7, 1949-M7.1, 1999-M7.4, and 1999-M7.1) of the series were irregular in the sense that they featured dominant eastward growth branches, which were probably of the  $-P_{SLOW}$  type.

The Parkfield earthquake sequence presents another interesting case in the context of bimaterial rupture. The slip is right-lateral, and the crust on the west side has faster wave speeds than on the east side (28). The two most recent Parkfield earthquakes ruptured the same section of the San Andreas fault. The rupture directions of the 1934 and the 1966 events were southeastward (positive direction), whereas the 2004 earthquake ruptured in the opposite direction (negative direction). Results from early constant friction coefficient studies in bimaterials (16, 17, 19, 20, 22, 23) implies that the positive (southeastward) direction of the 1934 and the 1966 events is a preferred direction. According to this notion, the negative (northwestward) direction of the 2004 earthquake would not be favored. However, our experiments have demonstrated that a rupture in the negative direction can occur.

**References and Notes**

1. R. J. Archuleta, *J. Geophys. Res.* **89**, 4559 (1984).
2. D. J. Wald, T. H. Heaton, *Bull. Seismol. Soc. Am.* **84**, 668 (1994).
3. M. Bouchon *et al.*, *Geophys. Res. Lett.* **28**, 2723 (2001).
4. M. Bouchon, M. Vallee, *Science* **301**, 824 (2003).
5. W. L. Ellsworth *et al.*, paper presented at the Eleventh International Conference of Soil Dynamics and Earthquake Engineering, Berkeley, California, 7 to 9 January 2004.
6. E. M. Dunham, R. J. Archuleta, *Bull. Seismol. Soc. Am.* **94**, S256 (2004).
7. K. Xia, A. J. Rosakis, H. Kanamori, *Science* **303**, 1859 (2004).
8. A. J. Rosakis, O. Samudrala, D. Coker, *Science* **284**, 1337 (1999).
9. A. J. Rosakis, *Adv. Phys.* **51**, 1189 (2002).
10. J. R. Rice, in *Mechanics for a New Millennium (Proceedings of the 20th International Congress of Theoretical and Applied Mechanics, 27 August to 2*

- September 2000)*, H. Aref, J. W. Phillips, Eds. (Kluwer, Chicago, 2001), pp. 1–23.
11. Y. Ben-Zion, *J. Mech. Phys. Solids* **49**, 2209 (2001).
12. S. M. Day, *Bull. Seismol. Soc. Am.* **72**, 1881 (1982).
13. D. J. Andrews, *J. Geophys. Res.* **81**, 5679 (1976).
14. A. Anooshehpour, J. N. Brune, *Geophys. Res. Lett.* **26**, 2025 (1999).
15. J. J. McGuire, L. Zhao, T. H. Jordan, *Bull. Seismol. Soc. Am.* **92**, 3309 (2002).
16. K. Ranjith, J. R. Rice, *J. Mech. Phys. Solids* **49**, 341 (2001).
17. A. Cochard, J. R. Rice, *J. Geophys. Res.* **105**, 25891 (2000).
18. G. G. Adams, *J. Appl. Mech.* **68**, 81 (2001).
19. J. Weertman, *J. Geophys. Res.* **85**, 1455 (1980).
20. D. J. Andrews, Y. Ben-Zion, *J. Geophys. Res.* **102**, 553 (1997).
21. Y. Ben-Zion, Y. Q. Huang, *J. Geophys. Res.* **107**, 10.1029/2001JB000254 (2002).
22. G. G. Adams, *J. Appl. Mech. Trans. ASME* **62**, 867 (1995).
23. G. G. Adams, *J. Appl. Mech. Trans. ASME* **65**, 470 (1998).
24. R. A. Harris, S. M. Day, *Bull. Seismol. Soc. Am.* **87**, 1267 (1997).
25. R. A. Harris, J. F. Dolan, R. Hartleb, S. M. Day, *Bull. Seismol. Soc. Am.* **92**, 245 (2002).
26. Bimaterial contrast is one of the two reasons cited in an attempt to explain bilateral rupture asymmetry for Izmit (3). However, as correctly pointed out by Andrews (29) and by Weertman (30), Bouchon *et al.* (3) assume that the higher wave speed material lies to the south of the fault, which is inconsistent with a westward growing +GR rupture. The present experiments conclusively settle the issue provided that the material to the north is the higher wave speed solid. However, if the fault is hypothesized to be homogeneous (3, 31), the rupture velocity asymmetry may alternatively be attributed to differences in fault plane morphology to the west (rough) and to the east (smooth) of the hypocenter.
27. E. Zor *et al.*, *Geophys. Res. Lett.* **30**, 10.1029/2003GL018129 (2003).
28. C. Thurber *et al.*, *Geophys. Res. Lett.* **30**, 10.1029/2002GL016004 (2003).
29. D. J. Andrews, *Geophys. Res. Lett.* **29**, 10.1029/2001GL014126 (2002).
30. J. Weertman, *Geophys. Res. Lett.* **29**, 10.1029/2001GL013916 (2002).
31. M. Bouchon, A. J. Rosakis, *Geophys. Res. Lett.* **29**, 10.1026/2002GL015096 (2002).
32. A.R., H.K., and K.X. acknowledge the support of NSF EAR 0207873 and Office of Naval Research N00014-03-0435. J.R. acknowledges the support by NSF EAR 0125702.

2 December 2004; accepted 16 February 2005  
10.1126/science.1108193